Springer

KSME

Journal of Mechanical Science and Technology 30 (11) (2016) 4877~4885
www.springerlink.com/content/1738-494x(Print)/1976-3824(Online)
DOI 10.1007/s12206-016-1006-8

Parametric study on a collocated PZT beam vibration absorber and power harvester†

Shyh-Chin Huang[1,2,*], Chao-Yang Tsai[3] and Hsiao-Hui Liao[4]

[1]*Mechanical Engineering, Ming Chi University of Technology, No. 84, Gongzhuan Rd., Taishan Dist., New Taipei City 24301, Taiwan*
[2]*College of Engineering, Chang Gung University, Taoyuan, Taiwan*
[3]*Mechanical Engineering, Army Academy, R.O.C., Taiwan, No. 750, 3rd Neighborhood, Longdong Rd. Zhongli Dist., Taoyuan City 32093, Taiwan*
[4]*LNG Construction & Project Division, CPC Corp., Taiwan*

(Manuscript Received February 1, 2016; Revised June 2, 2016; Accepted June 12, 2016)

Abstract

The parametric effects of a PZT beam that is simultaneously used as a vibration absorber and a power harvester were investigated in this study. A cantilever beam paved with PZT layers and with added tip mass has been widely used as a harvester or sometimes as a Dynamic vibration absorber (DVA). However, the beam is rarely considered a collocated device. In this study, the first step was theoretical derivation of a distributed beam covered with bimorph PZT layers. Then, the beam was attached to a 1DOF vibratory main system. Two indicators for vibration absorption and power harvesting were defined. Numerical results demonstrated that the lumped mass ratio favored both of the abilities, but that the DVA mass ratio influenced these two abilities in exactly the opposite way. The conjunction of a harvester circuit into a DVA shifted its resonance frequency up to 5 % (an extreme case of open circuit $R\rightarrow\infty$). Simultaneous power harvesting diminished the absorption capability up to 35 % for each set of mass ratios. To achieve the maximum degree of power harvesting, a corresponding load resistance that somewhat increases with the lumped mass ratio is applied. Experimental results verified the existence of the best load resistance, but the measured harvested curve was lower than the theoretical calculation because of structure damping and deviations of PZT material properties.

Keywords: Dynamic vibration absorber (DVA); Power harvester; PZT beam; Collocated DVA/harvester

1. Introduction

Mechanical vibration accompanies machine operation and must be eliminated when possible. Engineers have used either isolators or absorbers to attenuate vibrations. The most commonly used Dynamic vibration absorber (DVA) is 1DOF passive Spring-mass-damper (SMD) composition [1]. This type of DVA, which is also called Tuned vibration absorber (TVA) or Tuned mass damper (TMD), is mainly designed to attenuate single-frequency (tonal) vibration when connected to a main mass. The damper may be hooked to the ground instead of the main mass; this process is called ground-hook/sky-hook for enhanced absorption of base excitation [2, 3]. As regards the multi-frequency absorber, Sun et al. [4] placed two DVAs for two-frequency absorption and searched for optimal design parameters. They conclude that the easiest design is to tune the two DVAs to the two specific frequencies. Although this design is not the optimal solution, it is close to being optimal. Huang and Lin [5] designed a dual beam absorber that is interconnected with a spring for multi-frequency excitation. The most significant feature of that design is its ability to attenuate integer multiples of the base frequency, thereby making it suitable for periodic excitation. Hartog [6] and Snowdon [7] proposed the equal-peak approach to develop a SMD broader band; this approach has long been treated as the fundamental DVA design. Burdisso and Heilmann [8] replaced the DVA mass by a two-mass system that is interconnected with a damper, which could be a passive, semi-active, or active element. They experimentally tested that the vibration reduction was 3.7 times better than a conventional SMD and that the absorption band was significantly wider. A passive SMD DVA has limits regardless of the elaborate nature of the designs. Therefore, the latest developments of DVA mostly focus on semi-active or active devices. Sun et al. [9] surveyed the types of passive, semi-active, and active DVAs up to 1995. Sun et al. [10] compared the performance of passive, adaptive-passive, and hybrid types of 1DOF DVA. Their findings show that when compared against the passive type, the adaptive-passive type increases by 30 dB and the hybrid type increases by up to 50 dB.

The absorbed energy from vibration attenuation is usually

*Corresponding author. Tel.: +886 2 2908 9899(#4563), Fax.: +886 2 2906 3269
E-mail address: schuang@mail.mcut.edu.tw
† Recommended by Associate Editor Cheolung Cheong

dissipated into the environment by a damper. Retrieving and reusing the wasted energy has been a research topic in engineering for the last two decades. This branch of research is called energy/power harvesting; it has become a promising field in vibration engineering because of the advances in piezoelectric material development. Sodano et al. [11] categorized power harvesting studies into the following four groups: (1) Mechanical vibration, (2) power harvesting efficiency, (3) implantable and wearable power supplies, and (4) damping effect of power harvesting. Therefore, power harvesting from mechanical vibration is anticipated to be very promising in the future. Among all types of mechanical vibration harvesters, a PZT cantilever beam with a tip mass [12-14] is the most commonly used. This type of device has also been used as a tonal DVA. However, it is rarely considered a collocated DVA/harvester. To the best of our knowledge, the reason is that vibration absorption and energy harvesting have commonalities and differences. One such commonality is that both devices are designed to have the same resonance frequency as the main system. A 1DOF DVA is tuned to the main system's natural frequency so that it turns the main system's resonance into anti-resonance, thereby drastically reducing the base motion. A vibration harvester is designed to vibrate resonantly with the base system to harvest the most energy.

The differences are as follows: a DVA by nature diminishes the base motion for which it is named. However, the harvester is commonly assumed to not change the base vibration to which it is attached. This assumption is valid only if the mass ratio of the harvester to the main mass is reasonably small [15]; otherwise, its influence, called the damping effect, must be considered. A DVA attenuates the vibration amplitude of the base and consequently diminishes the possible power harvesting. The harvesting circuit, which is necessary for energy storage, somewhat changes the tuned frequency of the DVA [16] because of the shunt damping effect, thereby resulting in less absorption effectiveness. These mutual interferences make a collocated device difficult to design. In this study, we aim to investigate the parametric effects on the functions of absorption and harvesting, as well as search for appropriate designs for a collocated PZT beam DVA/harvester. We hope that the results provide useful information to vibration engineers.

2. Equations of motion

A PZT beam with a tip mass, as shown in Fig. 1, can be a DVA, an energy harvester, or both (collocated). The PZT layers are covered on the beam's two surfaces from root to L_{PZT} (partial coverage). The tip mass is used to enlarge the vibration amplitude because the harvested energy is proportional to the vibration amplitude. The first frequency of the set is tuned to the one to be attenuated, which is usually the natural frequency of the main system, as a DVA. The PZT layers are used to convert strain energy into electrical energy for power harvesting. This device, which is attached to a main system (1DOF SMD), is schematically shown in Fig. 2 and

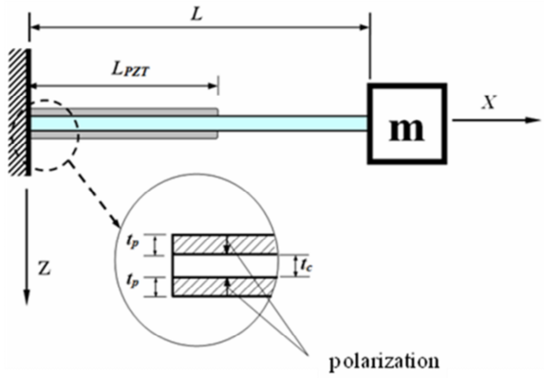

Fig. 1. Schematic of the PZT beam DVA/harvester.

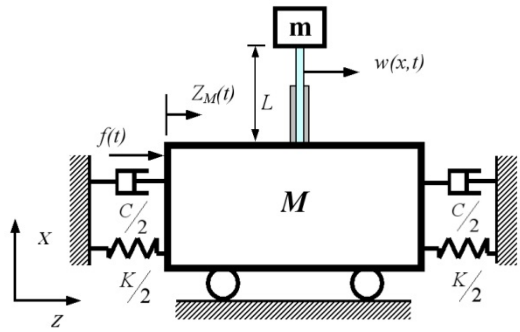

Fig. 2. 1DOF system connected to the DVA device.

the governing equations of the combined system are derived via Hamilton's principle and the assumed-mode process as [17]

$$[M]\{\ddot{q}\}+[C]\{\dot{q}\}+[K]\{q\}=\{F\} \tag{1}$$

where

$$[M]=\begin{bmatrix} M_T & \{m_i\}^T & 0 \\ \{m_i\} & [m_{ij}] & \{0\} \\ 0 & \{0\}^T & 0 \end{bmatrix},\ [C]=\begin{bmatrix} c & \{0\}^T & 0 \\ \{0\} & [c_{ij}] & \{0\} \\ 0 & \{0\}^T & 0 \end{bmatrix},\quad [K]=\begin{bmatrix} k & \{0\}^T & 0 \\ \{0\} & [k_{ij}] & \{k_i\} \\ 0 & -\{k_i\}^T & C_p \end{bmatrix} \tag{2}$$

$$M_T = M + m + b(\rho_b t_b L + 2\rho_p t_p L_{PZT}), \tag{3}$$

$$m_i = b\rho_b t_b \int_0^L \phi_i(x)dx + 2b\rho_p t_p \int_0^{L_{PZT}} \phi_i(x)dx + m\phi_i(L), \tag{4}$$

$$m_{ij} = b\rho_b t_b \int_0^L \phi_i(x)\phi_j(x)dx + 2b\rho_p t_p \int_0^{L_{PZT}} \phi_i(x)\phi_j(x)dx + m\phi_i(L)\phi_j(L), \tag{5}$$

$$c_{ij} = c_b \int_0^L \phi_i(x)\phi_j(x)dx, \tag{6}$$

$$k_{ij} = E_b I_b \int_0^L \phi_i''(x)\phi_j''(x)dx + 2\hat{A}\int_0^{L_{PZT}} \phi_i''(x)\phi_j''(x)dx, \tag{7}$$

$$k_i = \frac{1}{2}e_{31}b\left(t_b+t_p\right)\int_0^{L_{PZT}} \phi_i''(x)dx, \tag{8}$$

$$\{q\}^T = \{Z_M, \{\eta\}^T, V\}\,, \tag{9}$$

$$\{\eta_i\}^T = \{\eta_1(t), \eta_2(t), \ldots, \eta_n(t)\}\,, \tag{10}$$

$$\{F\}^T = \{f, \{0\}^T, Q\}\,, \tag{11}$$

$$\hat{A} = \frac{1}{3} b\left(c_{11}^E + \frac{e_{31}^2}{\varepsilon_{33}^S}\right)\left[\left(\frac{t_b}{2} + t_p\right)^3 - \left(\frac{t_b}{2}\right)^3\right] - \frac{e_{31}^2 b}{4 t_p \varepsilon_{33}^S}\left(t_b t_p + t_p^{\ 2}\right)^2, \tag{12}$$

$$C_p = \frac{\varepsilon_{33}^S b}{2 t_p} L_{PZT}\,. \tag{13}$$

$\phi_i(x)'s$ represents the exact mode shape of a cantilevered beam with a tip mass. The subscripts p and b represent the PZT and beam layers, respectively. All of the symbols are, as customarily defined, described in the Nomenclature section. Given that the exact beam modes are chosen for discretization, one mode approximation for low-frequency response is usually sufficient, i.e., by taking $\phi_1(x)$ only, then Eq. (1) is simplified to be

$$\begin{bmatrix} M_T & m_1 & 0 \\ m_1 & m_{11} & 0 \\ 0 & 0 & 0 \end{bmatrix}\begin{Bmatrix} \ddot{z}_M \\ \ddot{\eta}_1 \\ \ddot{V} \end{Bmatrix} + \begin{bmatrix} c & 0 & 0 \\ 0 & c_{11} & 0 \\ 0 & 0 & 0 \end{bmatrix}\begin{Bmatrix} \dot{z}_M \\ \dot{\eta}_1 \\ \dot{V} \end{Bmatrix} + \begin{bmatrix} k & 0 & 0 \\ 0 & k_{11} & k_1 \\ 0 & -k_1 & C_p \end{bmatrix}\begin{Bmatrix} z_M \\ \eta_1 \\ V \end{Bmatrix} = \begin{Bmatrix} f \\ 0 \\ Q \end{Bmatrix}. \tag{14}$$

Prior to working on the combined system, Eq. (14), the separate derivation of the PZT beam harvester alone is helpful in marking the two frequencies that are associated with a harvester, namely, the short-circuit and the open-circuit frequencies. The beam harvester equations, extracted from Eq. (14), are written as

$$\begin{bmatrix} m_{11} & 0 \\ 0 & 0 \end{bmatrix}\begin{Bmatrix} \ddot{\eta}_1 \\ \ddot{V} \end{Bmatrix} + \begin{bmatrix} c_{11} & 0 \\ 0 & 0 \end{bmatrix}\begin{Bmatrix} \dot{\eta}_1 \\ \dot{V} \end{Bmatrix} + \begin{bmatrix} k_{11} & k_1 \\ -k_1 & C_p \end{bmatrix}\begin{Bmatrix} \eta_1 \\ V \end{Bmatrix} = \begin{Bmatrix} g \\ Q \end{Bmatrix}, \tag{15}$$

where *g(t)* is the base excitation input at the beam's $x = 0$ end (base vibration), which is an internal force and does not need to be solved when the combined system is solved as a whole (Eq. (14)). The first row of Eq. (15) can be rewritten as

$$\frac{m_{11}}{k_1}\frac{\partial^2 w(L,t)}{\partial t^2} + \frac{c_{11}}{k_1}\frac{\partial w(L,t)}{\partial t} + \frac{k_{11}}{k_1} w(L,t) + V(t) = \frac{g(t)}{k_1}\cdot \phi_1(L)\,. \tag{16}$$

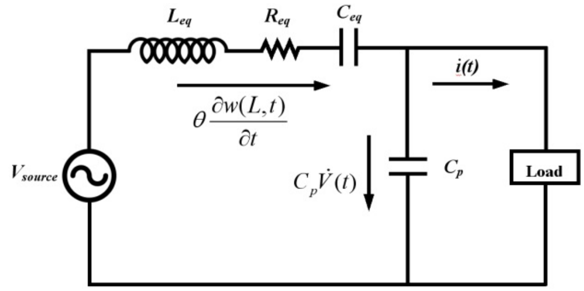

Fig. 3. Equivalent circuit diagram with harvester resistance.

One-term approximation for beam deflection is used, so that $w(L,t) = \eta_1(t)\phi_1(L)$ is applied. We rearrange Eq. (16) into an analogy of circuit equation [18, 19] as

$$L_{eq}\frac{di}{dt} + R_{eq} i + C_{eq}\int i dt + V(t) = \frac{g(t)}{k_1}\cdot \phi_1(L) = V_{source}\,, \tag{17}$$

where

$$i = \frac{k_1}{\phi_1(L)}\cdot\frac{\partial w(L,t)}{\partial t} = \theta\cdot\frac{\partial w(L,t)}{\partial t}\,, \tag{18}$$

$$L_{eq} = \frac{m_{11}}{k_1^2},\ R_{eq} = \frac{c_{11}}{k_1^2},\ C_{eq} = \frac{k_{11}}{k_1^2}\,, \tag{19}$$

where L_{eq}, R_{eq} and C_{eq} are the equivalent inductance, resistance, and capacity, respectively. ω_{sc} and ω_{oc} represent the short-circuit and open-circuit resonance frequency, and can be calculated based on Eq. (17) as

$$\omega_{sc} = \sqrt{1/L_{eq}C_{eq}}\,,\ \ \omega_{oc} = \sqrt{1/L_{eq}C_{eq} + 1/L_{eq}C_p}\,,\quad \frac{\omega_{oc}}{\omega_{sc}} = \sqrt{1 + C_{eq}/C_p}\,. \tag{20}$$

Numerous circuitry designs have been used for electrical energy storage [19-24]. The circuitry design is not discussed in the present study; thus, the harvested energy is simply represented by an external load resistance *R*, as shown in Fig. 3. The harvested energy is assumed to be retrieved by the load resistor *R* for computational simplicity. $V(t) = i(t)\cdot R = \dot{Q}(t)\cdot R$ so that the second equation of Eq. (15) can be rewritten as

$$-k_1\eta_1 + RC_p\dot{Q} - Q = 0\,. \tag{21}$$

By replacing the third equation in Eq. (14) by Eq. (21) and changing the variable *V* to electrical charge *Q*, Eq. (14) becomes

$$\begin{bmatrix} M_T & m_1 & 0 \\ m_1 & m_{11} & 0 \\ 0 & 0 & 0 \end{bmatrix} \begin{Bmatrix} \ddot{z}_M \\ \ddot{\eta}_1 \\ \ddot{Q} \end{Bmatrix} + \begin{bmatrix} c & 0 & 0 \\ 0 & c_{11} & Rk_1 \\ 0 & 0 & RC_p \end{bmatrix} \begin{Bmatrix} \dot{z}_M \\ \dot{\eta}_1 \\ \dot{Q} \end{Bmatrix} + \begin{bmatrix} k & 0 & 0 \\ 0 & k_{11} & 0 \\ 0 & -k_1 & -1 \end{bmatrix} \begin{Bmatrix} z_M \\ \eta_1 \\ Q \end{Bmatrix} = \begin{Bmatrix} f \\ 0 \\ 0 \end{Bmatrix} . \quad (22)$$

3. Parametric studies on vibration absorption and energy harvesting

Eq. (22) governs the dynamic behavior of the system in Fig. 2. The main goal of this study is to investigate how the design parameters of a collocated device affect the ability of vibration absorption and energy harvesting. The present study assumes that vibration absorption is the main purpose and seeks the possibility of simultaneous vibration energy harvesting during vibration attenuation. The questions that arise are the following: Will the retrieved energy reduce the intended absorption ability? If yes, how significant is the reduction? The PZT beam, when hooked with a harvester circuit, inevitably shifts its resonance frequency because of the shunt damping effect. Subsequently, the beam deviates from the originally tuned frequency. The absorption ability is predicated to degrade with harvested vibration energy. In the next subsection, we discuss the significance of the interference between the two functions as well as how the parameters are decided.

3.1 Indicators of vibration absorption and power harvesting

Two indicators are defined to quantify the vibration absorption and power harvesting capability.

$$I_{\mathrm{abs}} = 10 \times \log_{10}\left(\left|Z_{\mathrm{M}}\right| / \left|Z_{\mathrm{NDVA}}\right|\right) , \quad (23)$$

$$I_{\mathrm{har}} = i_{\mathrm{rms}}^2 R / v_{\mathrm{PZT}} , \quad (24)$$

where $\left|Z_{\mathrm{M}}\right| / \left|Z_{\mathrm{NDVA}}\right|$ represents the main mass vibration amplitude with/without DVA, respectively. $i_{\mathrm{rms}}^2 R$, with i_{rms} as the root-mean-square current, denotes the harvested power in electrical form; and v_{pzt} is the total volume of the paved PZT layers. I_{har} denotes the harvested power per unit PZT volume. The units of these two indicators are dB and mW/cm^3, respectively. I_{abs} is negative and a smaller value indicates better absorption. I_{har} is positive and a larger value is better.

3.2 Parametric effects

The following four design variables are defined for the device:

$$\mu_1 = \frac{m}{M_{\mathrm{b}}}, \quad \mu = \frac{M_{\mathrm{b}} + m}{M_{\mathrm{b}}}, \quad \lambda = \frac{\varpi}{\omega_{\mathrm{main}}}, \quad R , \quad (25)$$

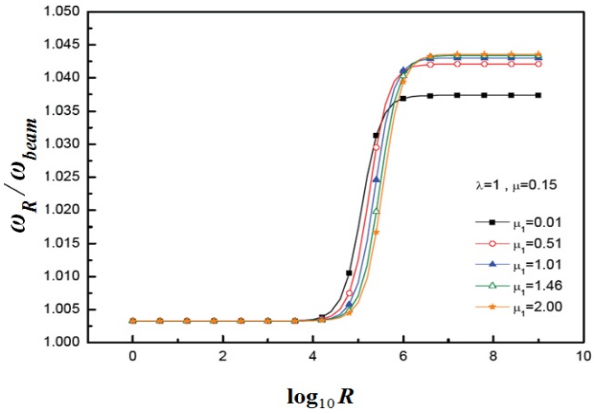

Fig. 4. Resonance frequency of device varies with load resistance.

where μ_1 is the lumped mass ratio, which is the ratio of tip mass (m) to beam mass (M_{b}); μ is the DVA mass ratio, which is the DVA's total mass over the main mass (M) ; λ :is the frequency ratio, which is the ratio of excitation frequency (ω) to the main system natural frequency (ω_{main}); and R is the load resistance. Considering the design viewpoint of both DVA and harvester, which indicates that the device frequency is tuned to that of the main system, the following studies focus only on the cases of $\lambda = 1$. Illustrations of two indicators that are subject to the variations of design parameters are discussed in this section. ω_{main} denotes the DVA's pure mechanical natural frequency without the PZT electrical effect, i.e., the piezoelectric terms are removed from the equations; ω_{R} denotes the resonance frequency of the collocated DVA/harvester, i.e., after the external circuit is hooked.

(i) Effects of lumped mass ratio μ_1 and load resistance R

A DVA mass is normally set below 20 % of the main mass to avoid significant alteration of system characteristics. Thus, the DVA mass ratio is, in the following examples, fixed at $\mu = 0.15$ (15 %) and μ_1 varies from 0.01, 0.51, 1.01, 1.46, to 2.00. The load is an adjustable resistance from 0 to $1\,G\Omega$. Larger μ_1 implies a larger tip mass (m) and smaller beam mass (M_{b}) because the total DVA mass is held constant (0.15 M). A larger μ_1 should induce larger beam vibration, but the fixed DVA natural frequency constraint, i.e., $\omega_{\mathrm{beam}} = \omega_{\mathrm{main}}$, results in a shorter/narrower beam with larger tip mass. The combined effects remain uncharted. Fig. 4 shows that the normalized resonance frequency ($\omega_{\mathrm{R}} / \omega_{\mathrm{beam}}$) varies with the harvester load resistance for various μ_1 ratios. At lower R, i.e., near short circuit (ω_{sc}) , the resonance frequency of the device hardly changes with μ_1 . This condition is understandable because of the lack of retrieved energy, and the DVA tuned frequency is not altered. However, this phenomenon changes as energy harvesting begins (increasing R). The resonance frequency increases with R and eventually approaches the open circuit frequency (ω_{oc}), which increases with μ_1 as well. Notably, ω_{R} is slightly larger than ω_{beam} , with a ratio of 1.0033 rather than 1.0 even with the short circuit. The difference is attributed to the piezoelectric effect in the PZT layers. The

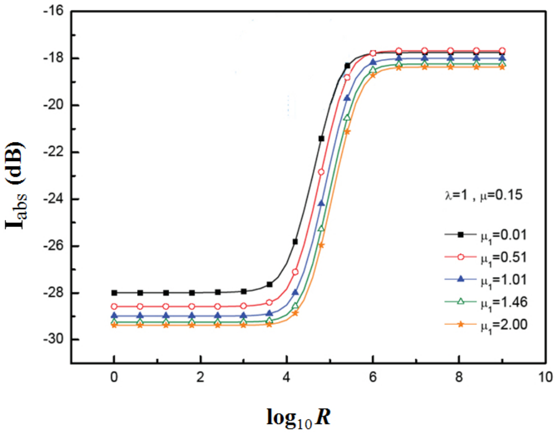

Fig. 5. I_{abs} varies with R for various μ_l.

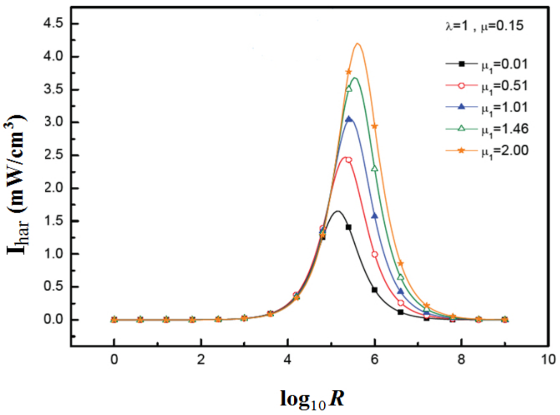

Fig. 6. I_{har} varies with R for various μ_l.

ω_R of the collocated device falls within $[\omega_{sc}, \omega_{oc}]$ when a harvesting circuit is connected; this range is roughly 5 %, depending on μ_1. The result is very close to the findings of other studies that showed a 6 % frequency shift [16].

Fig. 5 illustrates the absorption indicator versus load resistance for various μ_1 ratios. I_{abs} worsens with the increase of R because ω_R deviates more with an increased difference from the originally tuned frequency ω_{beam}. The decline could be as much as 11 dB for all cases of μ_1. As observed, larger lumped mass ratio μ_1 magnifies the absorption ability (lower curves). The capability increases by roughly 1.3 dB (4.6 %) as μ_1 changes from 0.01 to 2.00. The results explain that a larger tip mass increases the vibration amplitude, and therefore, stores more kinetic and strain energy in DVA. Similarly, Fig. 6 shows how R and μ_1 affect I_{har}. The best load resistance is found for every lumped mass ratio μ_1; the best R somewhat increases with μ_1. μ_1 influences I_{har} in a similar trend as I_{abs}, i.e., larger μ_1 induces a larger strain energy, which is then converted into electrical energy. Table 1 lists the peak values of I_{har} of Fig. 6 and the associated best R. By increasing the lumped mass ratio μ_1 from 0.014 to 2.00, I_{har} is lifted by 150 %.

Table 1. Best R and I_{har} for various μ_l with μ = 0.15.

μ_l	R(Ω)	I_{har} (mW/cm^3)
0.014	138.038 k	1.656
0.501	209.930 k	2.475
1.006	275.423 k	3.056
1.458	331.131 k	3.576
2.000	398.107 k	4.205

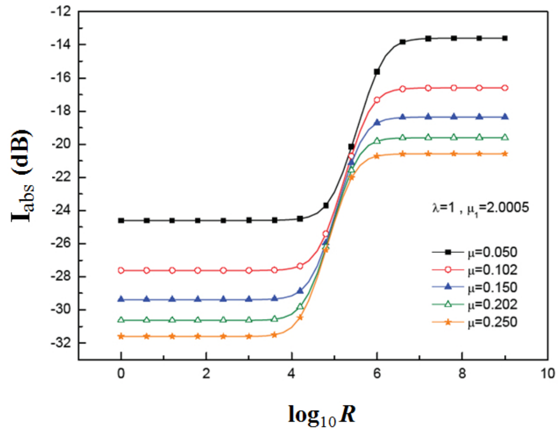

Fig. 7. I_{abs} varies with R for various μ.

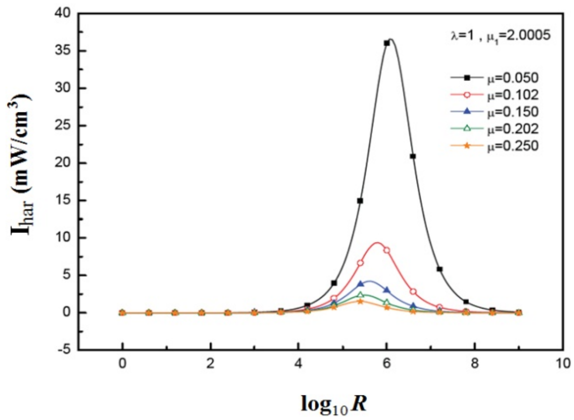

Fig. 8. I_{har} varies with R for various μ.

(ii) Effects of DVA mass ratio μ and load resistance R

Figs. 5 and 6 suggest that larger μ_1 benefits both absorption and harvesting abilities, so $\mu_1 = 2.0$ is fixed in the following discussion. The two indicators vary with R for different mass ratios μ as illustrated in Figs. 7 and 8. As shown in Fig. 7, a larger DVA mass ratio μ consistently yields better absorption; such a result is well known in DVA design. The difference, as shown in Fig. 7, can be up to 7 dB (29 %) as μ changes from 0.05 to 0.25. As expected, I_{abs} decreases with load resistance. One may infer, as observed from Figs. 5 and 7, that for any set of fixed (μ, μ_1) combination, I_{abs} drops by roughly 11 dB from short circuit ($R = 0$) to open circuit ($R = \infty$). The first conclusion may be drawn from the observation that the DVA may diminish by up to 35 % of its performance

Table 2. Best R and I_{har} for various μ_1 with μ = 2.0.

μ_1	R(Ω)	I_{har} (mW/cm^3)
0.050	1.202 M	36.664
0.102	619.4 k	9.387
0.150	398.1 k	4.205
0.202	302.0 k	2.375
0.250	242.1 k	1.524

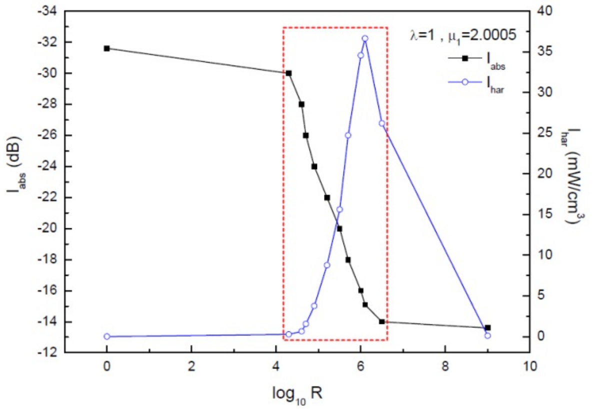

Fig. 9. Interactions between I_{abs} and I_{har} at various μ ratios and the associated best load resistance.

(31.6 to 20.6 dB) if the vibration energy is simultaneously harvested. As regards $I_{\rm har}$, Fig. 8 shows a completely opposite trend in which larger μ yields lower harvesting power. Table 2 shows the best values of R and their corresponding $I_{\rm har}$ for each μ .When μ increases from 0.05 to 0.25, the harvested power drops by 96 %. The growth and decline of two indicators, $I_{\rm abs}$ and $I_{\rm har}$, that are associated with the best R are shown in Fig. 9 and the data are listed in Table 3. The vibration attenuation could be as large as 31.6 dB if DVA is the only consideration by choosing $\mu = 0.25$, $\mu_1 = 2.0$ and R = 0. To achieve better absorption, μ and μ_1 can be chosen to be even larger but they should fall within the reasonable range. A maximum harvesting rate (with μ_1 fixed 2.0) of 36.65 mW/cm^3 can be obtained as $\mu = 0.05$, $R = 1.26$ MΩ. As a result, the DVA ability drops to 15.1 dB, which represents a compromise of 16.5 dB. The interactions between $I_{\rm abs}$ and $I_{\rm har}$, as shown in Fig. 9, indicate that reasonable load resistance falls within [20 k, 3 M]Ω. In this region, $I_{\rm abs}$ drops rapidly and $I_{\rm har}$ increases sharply. The squared region is used for appropriate parameter design when both absorption and harvesting are considered. The optimal solution may be obtained by appropriate weighting on two indicators based on the requirement. Fig. 10 shows the surfaces of two indicators as functions of μ and R. One red dot is marked on each plot to indicate the best performance of each function.

4. Experimental verification

A 1DOF spring-mass system and a PZT beam with tip mass are fabricated for the power harvesting test. The geometrical and material data of the test specimen are given in Table 4. Fig. 11 shows a photograph of the PZT beam, in which the PZT layer is paved from the clamped end to the middle of the beam. The theoretical and experimental frequencies by ham-

Table 3. Growth and decline between two indicators I_{abs} and I_{har} for μ_1 = 2.0.

I_{abs} (dB)	μ	R(Ω)	I_{har} (mW/cm^3)
-31.6	0.25	0	0
-30.0	0.25	19.95 k	0.25
-28.0	0.16	39.81 k	0.62
-26.0	0.10	50.12 k	1.54
-24.0	0.06	79.43 k	3.75
-22.0	0.05	158.49 k	8.76
-20.0	0.05	501.19 k	15.61
-18.0	0.05	794.33 k	24.74
-16.0	0.05	1 M	34.57
-15.1	0.05	1.26 M	36.65
-14.0	0.05	3.16 M	26.22
-13.6	0.05	1 G	0.09

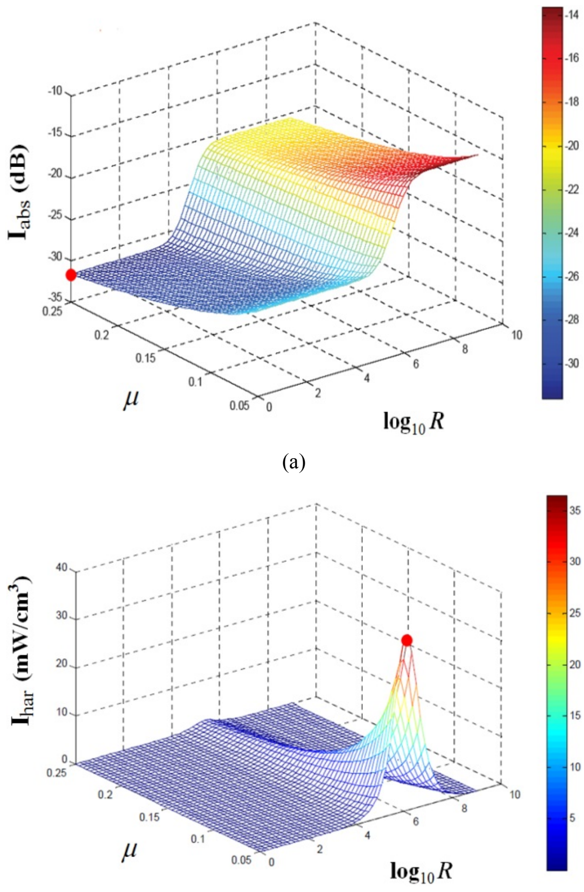

(a)

(b)

Fig. 10. Two indicators vary with DVA mass ratio.

Table 4. Parameters of the test specimen.

Geometrical parameters (*mm*)				
L_{beam}	L_{pzt}	t_b	t_p	b
80	40	0.5	0.7	10
Material properties				
$M(g)$	k (*N/m*)	m (*g*)	ρ_b (kg/m^3)	ρ_p (kg/m^3)
102.9	$6.622(10^3)$	5.83	$8.874(10^3)$	$7.266(10^3)$
c_b	E_c (*GPa*)	c_{11}^E (*GPa*)	ε_{33}^s (*F/m*)	e_{31} (C/m^2)
0	102	84	$9.5268(10^{-9})$	-8.4425

Table 5. Theoretical and experimental resonance frequencies.

Resonance frequency (Hz)	Theory	Experiment	Error
Spring-mass system	40.37	39.96	1.02 %
PZT beam + tip mass (short circuit)	41.65	40.4	3.09 %

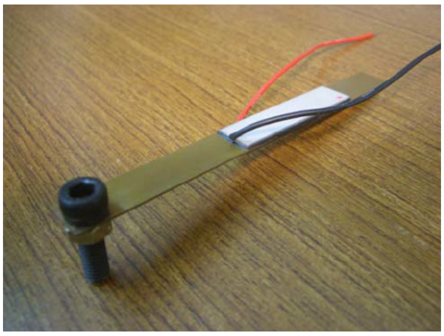

Fig. 11. Photograph of the partially covered PZT beam.

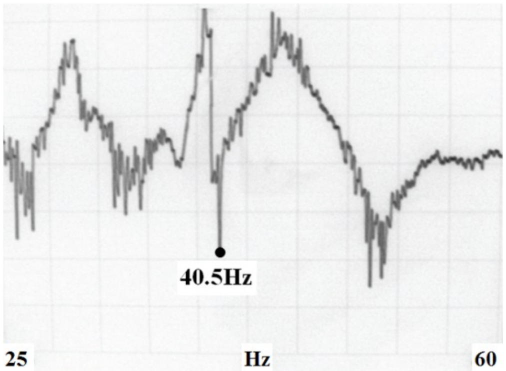

Fig. 12. FRF of the combined system.

mer impact test are shown in Table 5. The PZT beam showed a 3.09 % error. The beam's measured frequency is assumed as the actual one, $\omega_{beam} \approx \omega_{sc}$, and is taken as the excitation frequency in the harvesting test. The DVA is now fixed to the main mass; the FRF of the combined system is measured through a hammer test, as shown in Fig. 12. The system response shows an anti-resonance of 40.5 Hz that is very close to the tuned frequency of the DVA. The FRF indicates that the DVA operates as designed. An adjustable external resistance for power harvesting is connected to the PZT wire outs, and

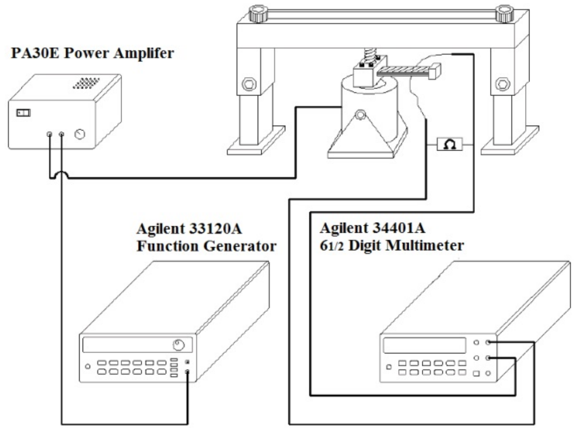

Fig. 13. Setup of the vibration energy-harvesting experiment.

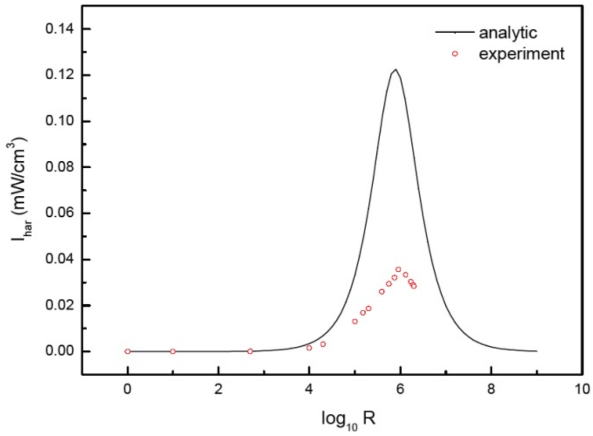

Fig. 14. Comparisons of theoretical and measured I_{har}.

then a sequence of harvested power is measured. Fig. 13 shows the schematic of experimental setup in which the shaker excites the main system (mass-spring) at various frequencies. The experimental results of harvested power are compared against the theoretical calculations in Fig. 14. The real harvested power is apparently lower than the calculations, but peak occurrence is extremely close to the theoretical prediction of R. Most importantly, both curves show a relatively consistent trend, thereby validating the derived theory to be appropriate. The error, in our opinion, is attributable to the following reasons: (1) The damping in the structure and environment is not included in theoretical analysis, (2) all calculations were based on $\lambda = 1$ but the main system's frequency was slightly different from the excitation frequency so that $\lambda = 1.001$, and (3) the piezoelectrical constants of the fabricated PZT layers may not closely match the listed values.

5. Conclusions

A collocated device of the DVA/harvester was investigated. Two indicators to quantify the vibration absorption and energy harvesting ability were defined and the effects of various parameters on these two indicators were studied. The theoretical results showed that sacrifice of vibration absorption is inevitable if the vibration energy is simultaneously harvested. Numerical calculations indicated that the DVA's resonance frequency increased by roughly 5 % from short circuit to open circuit, and the absorption capability could drop by as much as 35 % for every fixed set of (μ_1, μ). An increase in the lumped mass ratio favors both the absorption and harvesting capabilities because a larger tip mass magnifies the beam's vibration amplitude; thus, a larger amount of energy is extracted from the main system such that both the vibration attenuation and energy harvesting increase. A larger DVA mass ratio, as well known in DVA design, increases the absorption ability and reduces the sensitivity to frequency variation. The opposite effect of energy harvesting has yet to be determined, i.e., a smaller DVA mass ratio induces larger harvested energy in electrical form. The reason is that a larger mass ratio extracts more energy from the main system and is stored into the DVA's kinetic energy such that it enhances the absorption capability. However, the harvested energy is converted from the beam's strain energy, not from the kinetic energy. A larger DVA mass under a fixed frequency constraint apparently results in a stiffer beam so that the beam deflection becomes even smaller. Such a result explains the reduction of harvested power with the increase of DVA mass ratio.

The harvested power is assumed by a load resistor, which is a more sophisticated circuitry with appropriate electrodes that are required in applications, to store usable electrical energy. The simulations show that the best resistance value exists for every set of parameters. The experiment verified the occurrence of best load resistance and curve shape, but the harvested powers were smaller than the theoretical calculations. The error is mainly due to the existence of damping in the structure; another possible reason is the inaccuracy of the piezoelectric constants of the test specimen.

Acknowledgment

The authors appreciate the support of the Ministry of Science and Technology of Taiwan under Grant NSC102-2221-E-131-014.

Nomenclature

b : Beam width
c : Main system damping coefficient
c_b : Beam's equivalent damping coefficient
E_i : Young's modulus
f : Excitation force to main system
I_{abs} : Absorption indicator
I_{har} : Harvesting indicator
$I(t)$: Harvested current
k : Main system stiffness
L : Beam length
L_{PZT} : PZT layer length
M : Main system mass
M_T : Combined system total mass
M_b : Beam mass
m : Lumped tip mass
Q : Electrical charge
R : Load resistance
q_i : Generalized coordinates
t_i : Thickness
t_b : Beam thickness
t_p : PZT layer thickness
V : PZT layer's total differential voltage
v_{PZT} : PZT layer's total volume
$w(x,t)$: Beam transverse displacement
Z_M : Main system response amplitude
Z_{NDVA} : Response amplitude without DVA
Z_{st} : Main system static displacement
$\varphi_i(x)$: Beam modes
$\eta_i(t)$: Beam modal participation factors
λ : Driving frequency ratio ω/ω_{main}
μ : DVA mass ratio $(m+M_b)/M$
μ_1 : Lumped mass ratio m/M_b
ρ_i : Density
ρ_b : Beam density
ρ_p : PZT layer density
ω : Excitation frequency
ω_{beam} : DVA's mechanical natural frequency
ω_{main} : Main system natural frequency $(K/M)^{1/2}$
ω_{oc} : Harvester's open circuit frequency
ω_R : Harvester's resonance frequency
ω_{sc} : Harvester's short circuit frequency

Subscripts

b : Core layer (beam)
p : PZT layer

PZT material coefficients

c_{ij}^E : Stiffness coefficient
ε_{ij}^S : Dielectric constant
e_{ij} : Charge-stress constant

References

[1] F. Hermann, Device for damping vibration of bodies, *German Patent No. 525455* (1909).
[2] M. Z. Ren, A variant design of the dynamic vibration absorber, *J. Sound Vib.*, 245 (4) (2001) 762-770.
[3] K. Lih and J. Liu, The damped dynamic vibration absorbers: revisited and new result, *J. Sound Vib.*, 284 (2005) 1181-1189.
[4] H. L. Sun, P. Q. Zhang, H. B. Chen and X. L. Gong, Application of dynamic vibration absorbers in structural vibration control under multi-frequency harmonic excitation, *Applied Acoustics,* 69 (2008) 1361-1367.
[5] S. C. Huang and K. A. Lin, A new design of vibration ab-

sorber for periodic excitation, *Shock and Vibration* (2014) Article ID 571421: 1-11.
[6] J. P. Den Hartog, *Mechanical vibration*, McGraw Hill, New York, USA (1956).
[7] J. C. Snowdon, *Vibration and shock in damped mechanical systems*, John Wiley & Sons, New York, USA (1968).
[8] R. A. Burdisso and J. D. Heilmann, A new dual-reaction mass dynamic vibration absorber actuator for active vibration control, *J. Sound Vib*., 214 (5) (1998) 817-831.
[9] J. Q. Sun, M. R. Jolly and M. A. Norris, Passive, adaptive and active tuned vibration absorbers-a survey, *ASME J. Mech. Des.,* 117 (1995) 234-242.
[10] H. L. Sun, P. Q. Zhang, X. L. Gong and H. B. Chen, A novel kind of active resonator absorber and the simulation on its control effort, *J. Sound Vib.,* 300 (2007) 117-125.
[11] H. A. Sodano, D. J. Inman and G. Park, A review of power harvesting from vibration using piezoelectric materials, *Shock Vib. Dig.,* 36 (2004) 197-205.
[12] J. E. Kim and Y. Y. Kim, Analysis of piezoelectric energy harvesters of a moderate aspect ratio with a distributed tip mass, *ASME J. Vib. Acoust.,* 132 (2011) 041010.
[13] M. Kim, M. Hoegen, J. Dugundji and B. L. Wardle, Modeling and experimental verification of proof mass effects on vibration energy harvester performance, *Smart Mater. Struct.,* 19 (2010) 045023.
[14] R. Patel, S. McWilliam and A. A. Popov, A geometric parameter study of piezoelectric coverage on a rectangular cantilever energy harvester, *Smart Mater. Struct.,* 20 (2011) 085004.
[15] M. Lallart, Y. C. Wu, L. Yan, C. Richard and D. Guyomar, The effect of seismic energy scavenging on host structure and harvesting performance, *Smart Mater. Struct.,* 22 (2013) 035009.
[16] S. Rafique and P. Bonello, Experimental validation of a distributed parameter piezoelectric bimorph cantilever energy harvester, *Smart Mater. Struct.,* 17 (2010) 094008.
[17] S. C. Huang and K. A. Lin, A novel design of map-tuning piezoelectric vibration energy, *Smart Mater. Struct.,* 21 (2012) 085014.
[18] Y. C. Shu and I. C. Lien, Analysis of power output for piezoelectric energy harvesting systems, *Smart Mater. Struct.,* 15 (2006) 1499-1512.
[19] Y. C. Shu and I. C. Lien, Array of piezoelectric energy harvesting by the equivalent impedance approach, *Smart Mater. Struct.,* 21 (2012) 082001.
[20] M. E. Poese, Performance measurements on a thermoacoustic refrigerator driven at high amplitudes, *M.S. Thesis*, Pennsylvania State University (1998).
[21] V. R. Challa, M. G. Prasad and F. T. Fisher, A coupled piezoelectric-electromagnetic energy harvesting technique for achieving increase power output through damping matching, *Smart Mater. Struct.,* 18 (2009) 095029.
[22] H. Shen, J. Qiu, H. Ji, K. Zhu and M. Balsi, Enhanced synchronized switch harvesting: a new energy harvesting scheme for efficient energy extraction, *Smart Mater. Struct.,* 19 (2010) 115017.
[23] Y. C. Shu, I. C. Lien and W. J. Wu, An improved analysis of the SSHI interface in piezoelectric energy harvesting, *Smart Mater. Struct.,* 16 (2007) 2253-2264.
[24] I. C. Lien, Y. C. Shu, W. J. Wu, S. M. Shiu and H. C. Lin, Revisit of series-SSHI with comparisons to other interfacing circuits in piezoelectric energy harvesting, *Smart Mater Struct.,* 19 (2010) 1255009.

Shyh-Chin Huang received an M.S. degree in Mechanical Engineering from the University of Iowa in 1984, and a Ph.D. degree in Mechanical Engineering from Purdue University in 1987. Dr. Huang is currently a Chair Professor and Researcher at Ming Chi University of Technology. His research interests are in the areas of vibration control, smart materials, electric shunt damping design, and reliability of Li-ion battery.